New Phytologist Supporting Information

Full title: Quantitative phosphoproteomic analysis reveals common regulatory mechanisms between effector- and PAMP-triggered immunity in plants

Authors: Yasuhiro Kadota, Thomas W.H. Liebrand, Yukihisa Goto, Jan Sklenar, Paul Derbyshire, Frank L.H. Menke, Miguel-Angel Torres, Antonio Molina, Cyril Zipfel, Gitta Coaker, Ken Shirasu

The article acceptance date: 1st OCT, 2018

Kadota & Liebrand et al., Figure S1

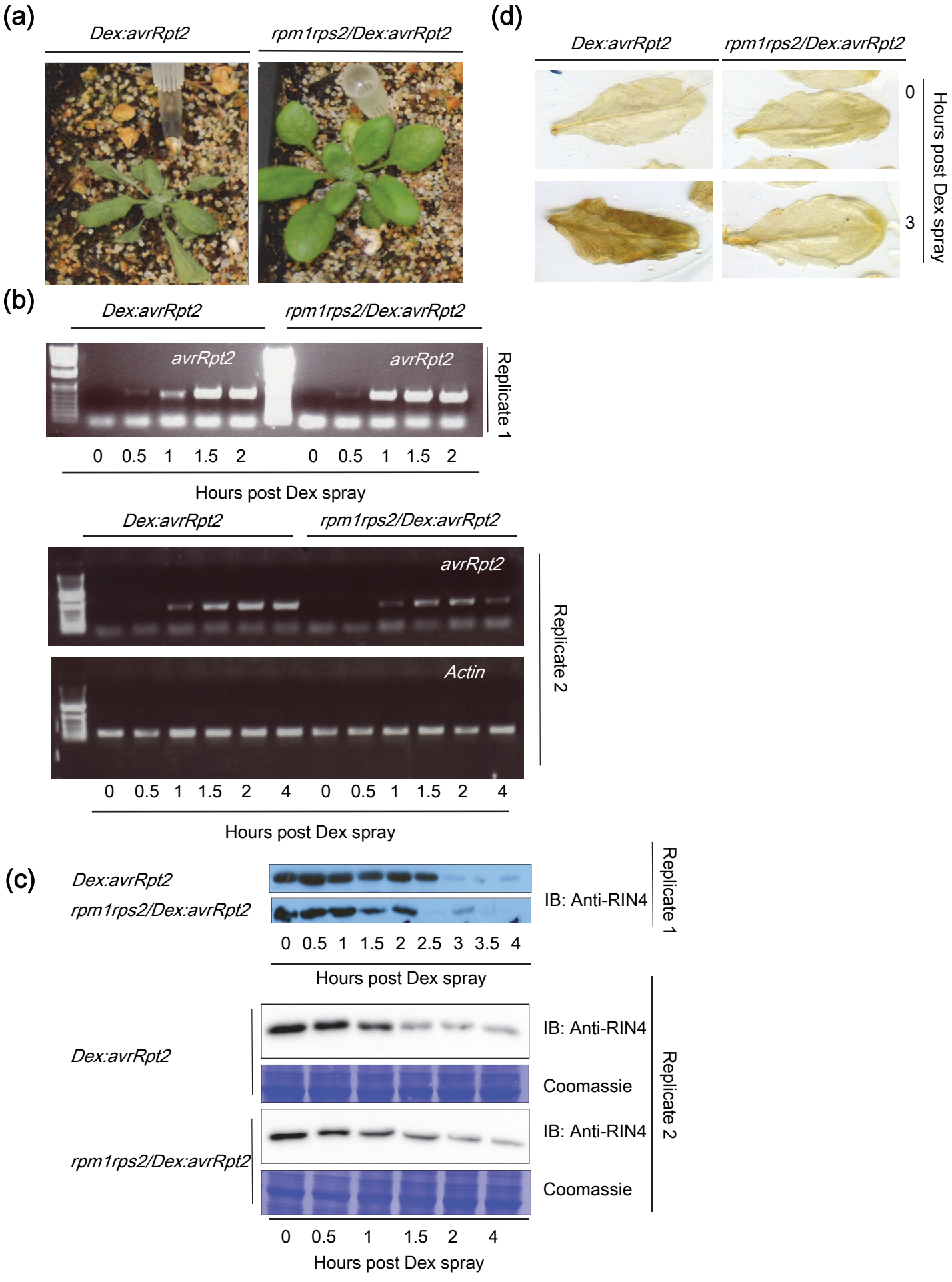

Fig. S1 Dexamethasone (Dex)-inducible *avrRpt2* expression in *Arabidopsis*. (a) Dex application to Col-0 *Dex:avrRpt2* plants results in visible cell-death and tissue collapse after 6-7 hours, while *rpm1rps2/Dex:avrRpt2* does not show cell death. Pictures were taken 7 hours post Dex application. (b) Semi-quantitative PCR analysis reveals Dex-induced *avrRpt2* expression as early as 0.5 hours after Dex application. Two replicate experiments representing a time series are shown, amplification of endogenous *Actin* was used as loading control in replicate 2 (c) Immunoblotting reveals AvrRpt2-mediated RIN4 degradation at 2-3 hours post Dex application. Two replicate experiments are shown, Coomasssie stain of blots shows the rubisco band to indicate equal protein loading. (d) AvrRpt2 induces H_2O_2 production in *Dex:avrRpt2* but not in *rpm1rps2/Dex:avrRpt2.* H_2O_2 accumulation is analyzed by 3,3'-diaminobenzidine (DAB) staining.

Kadota & Liebrand et al., Figure S2

(a)

```
AHA1(AT2G18960.1)859- AFTTKKDYGIGEREAQWAQAQRTLHGLQPKEDVNIFPEKGSYRELSEIAEQ
AHA2(AT4G30190.1)859- AFTMKKDYGKEEREAQWALAQRTLHGLQPKEAVNIFPEKGSYRELSEIAEQ
AHA3(AT5G57350.2)860- AFTTKQNYGIEEREAQWAHAQRTLHGLQNTETANVVPERGGYRELSEIANQ
AHA4(AT3G47950.1)871- AFTRQKDFGKEQRELQWAHAQRTLHGLQAP-DTKMFTDRTHVSELNQMAEE
                      *** :::::*  :** *** ********* .::..::       **.::*::

AHA1(AT2G18960.1)910- AKRRAEIARLRELHTLKGHVESVAKLKGLDIDTAGHHYTV
AHA2(AT4G30190.1)910- AKRRAEIARLRELHTLKGHVESVVKLKGLDIETP-SHYTV
AHA3(AT5G57350.2)911- AKRRAEIARLRELHTLKGHVESVVKLKGLDIETA-GHYTV
AHA4(AT3G47950.1)921- AKRRAEIARLRELHTLKGHVESVVRLKGLDIETIQQAYTV
                      **********************.:*******:*    ***
```

(b)

```
PIP2D(AT3G54820.1)251- WVGPFAGAAIAAFYHQFVLRAGAIKALGSFRSQPHV---
PIP2E(AT2G39010.1)251- WVGPFVGAAIAAFYHQFVLRAGAMKAYGSVRSQLHELHA
PIP3A(AT4G35100.2)245- WVGPFLGALAAAAYHQYILRASAIKALGSFRSNATN---
                       ***** **  ** ***::***.*:** **.**:
```

(c)

```
PIN3(AT1G70940.1)248- SDFYNMMGFPGGRLSNFGPADMYSVQSSRGPTPRPSNFEENCAMASSPRF
PIN4(AT2G01420.1)245- SDFYSVMGFPGGRLSNFGPADLYSVQSSRGPTPRPSNFEENNAVKYGFYN
PIN7(AT1G23080.2)251- SDFYSMMGFPGGRLSNFGPADMYSVQSSRGPTPRPSNFEESCAMASSPRF
                      ****.:***************:******************. *:  .
```

Fig. S2 Alignments of differentially phosphorylated sites in PIP, AHA and PIN proteins. Regions of differentially phosphosites of AHAs(a), PIPs(b) and PINs(c) were aligned using ClustalW. The residues in red are differentially phosphorylated residues after Dex treatment, whose total protein levels do not change significantly in abundance (see also Table S1). The residues in orange are differentially phosphorylated residues after dexamethasone treatment, for which total protein levels were not detected (see also Table S1). Identified phosphopeptides are underlined within the alignment (see also Table S6).

Kadota & Liebrand et al., Figure S3

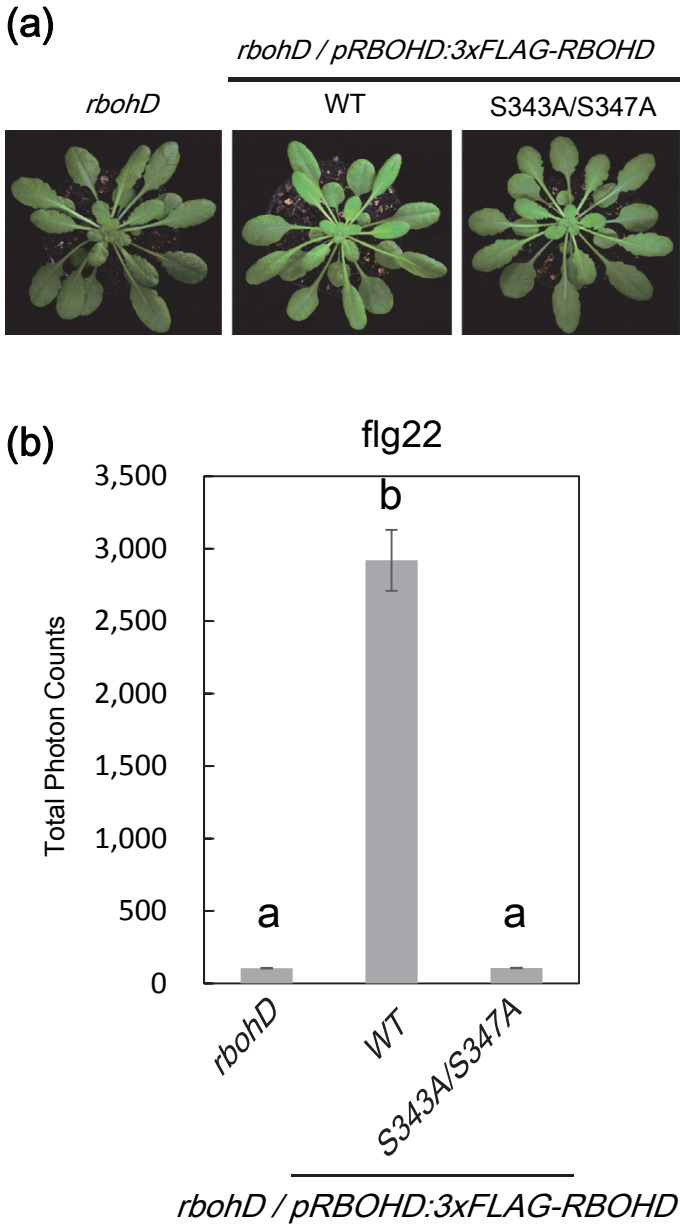

Fig. S3 RESPIRATORY BURST OXIDASE HOMOLOGUE D (RBOHD) phosphorylation sites S343 and S347 are required for flagellin 22 (flg22)-inducible reactive oxygen species (ROS) burst. (a) There is no growth phenotype in *rbohD* and *rbohD/pRBOHD:3xFLAG-RBOHD* (WT) and *rbohD pRBOHD:3xFLAG-RBOHD* (S343A/S347A) lines. (b) Phosphorylation of S343 and S347 is required for flg22-inducible ROS burst in *Arabidopsis*. Leaf discs were treated with 200 nM flg22 and the ROS production was measured over 40 min. Values are mean ±SE (n = 8). Different letters indicate significantly different values at $p \leq 0.001$ (one way ANOVA, Tukey post hoc test). The experiments were performed three times with similar results.

Kadota & Liebrand et al., Figure S4

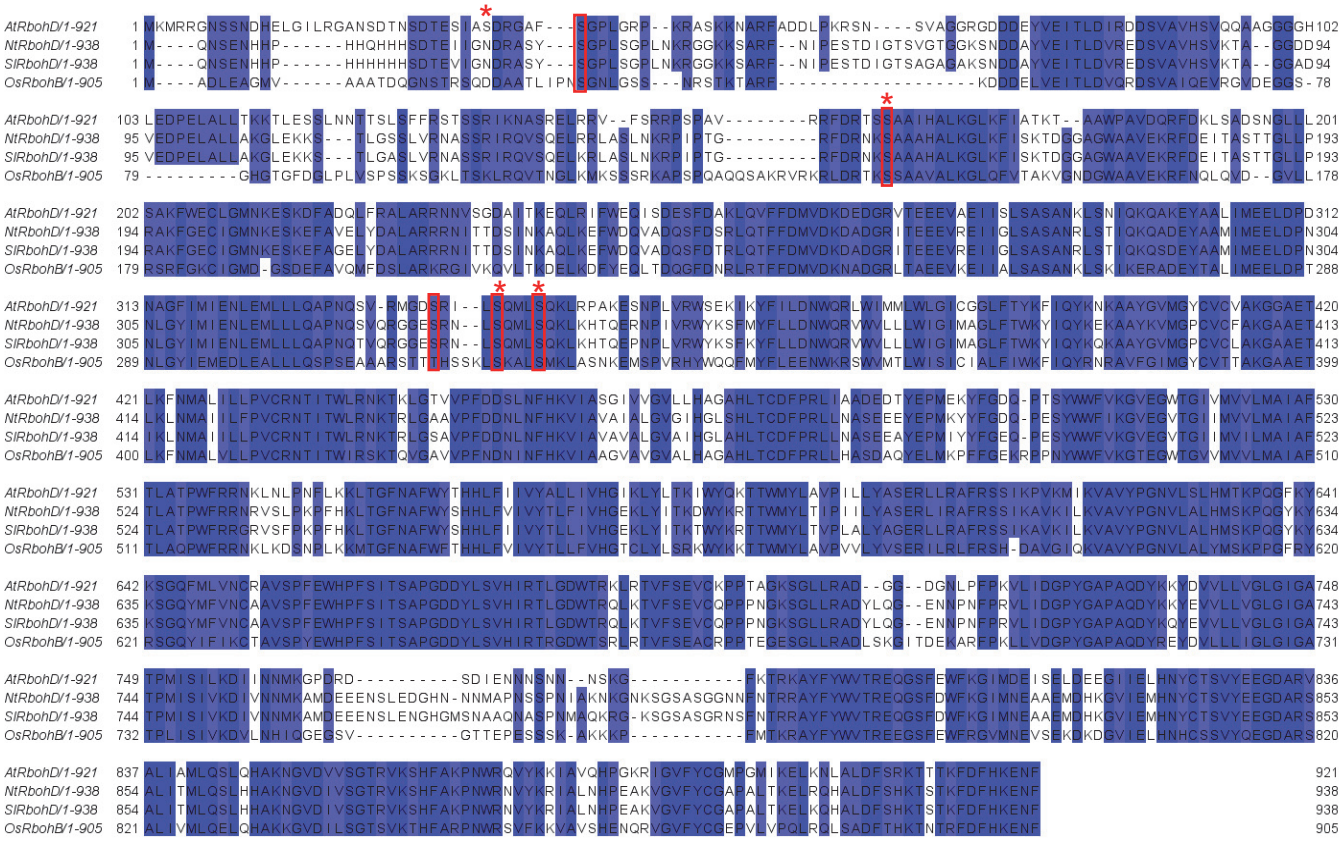

Fig. S4 Conservation of identified RESPIRATORY BURST OXIDASE HOMOLOGUE D (RBOHD) phosphorylation sites in the phosphoproteomic screen. An alignment of *Arabidopsis* RBOHD (AtRBOHD), *Nicotiana tabacum* RBOHD (NtRBOHD), *Solanum lycopersicum* RBOHD (SlRBOHD) and the rice RBOHD ortholog *Oryza sative* RBOHB (*Os*RBOHB) is provided. Phosphorylation sites whose phosphorylation were significantly upregulated after dexamethasone treatment (one-way ANOVA+T-test p≤0.05) are shown with asterisks. Phosphorylation sites identified as differentially phosphorylated during PTI in previous studies are indicated with a square red box.

Kadota & Liebrand et al., Figure S5

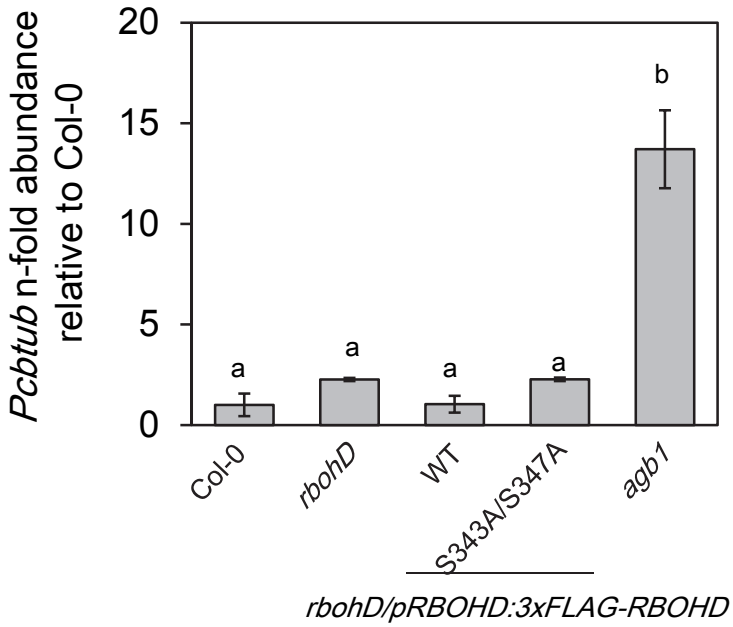

Fig. S5 The *rbohD/pRBOHD:3xFLAG-RBOHD* (S343A/SS347A) complementation line is resistant to *Plectosphaerella cucumerina* (*PcBMM* isolate). Quantification of fungal biomass 5 dpi after spray inoculation with *PcBMM* isolate (4 x 10^6 spores/ml) on 18 day old plants. Fungal DNA (*Pc*β-tubulin) was quantified by qPCR using specific primers for *Pcβ-TUBULIN* and normalized to Arabidopsis *UBIQUITIN10*. Bars represent averages (±SE) of fungal DNA levels relative to Col-0 plants, from one of two independent repetitions of the assay. Statistical analysis was performed by ANOVA , corrected with Bonferroni post hoc test. Different letters indicate significant differences ($p \leq 0.05$).

Kadota & Liebrand et al., Figure S6

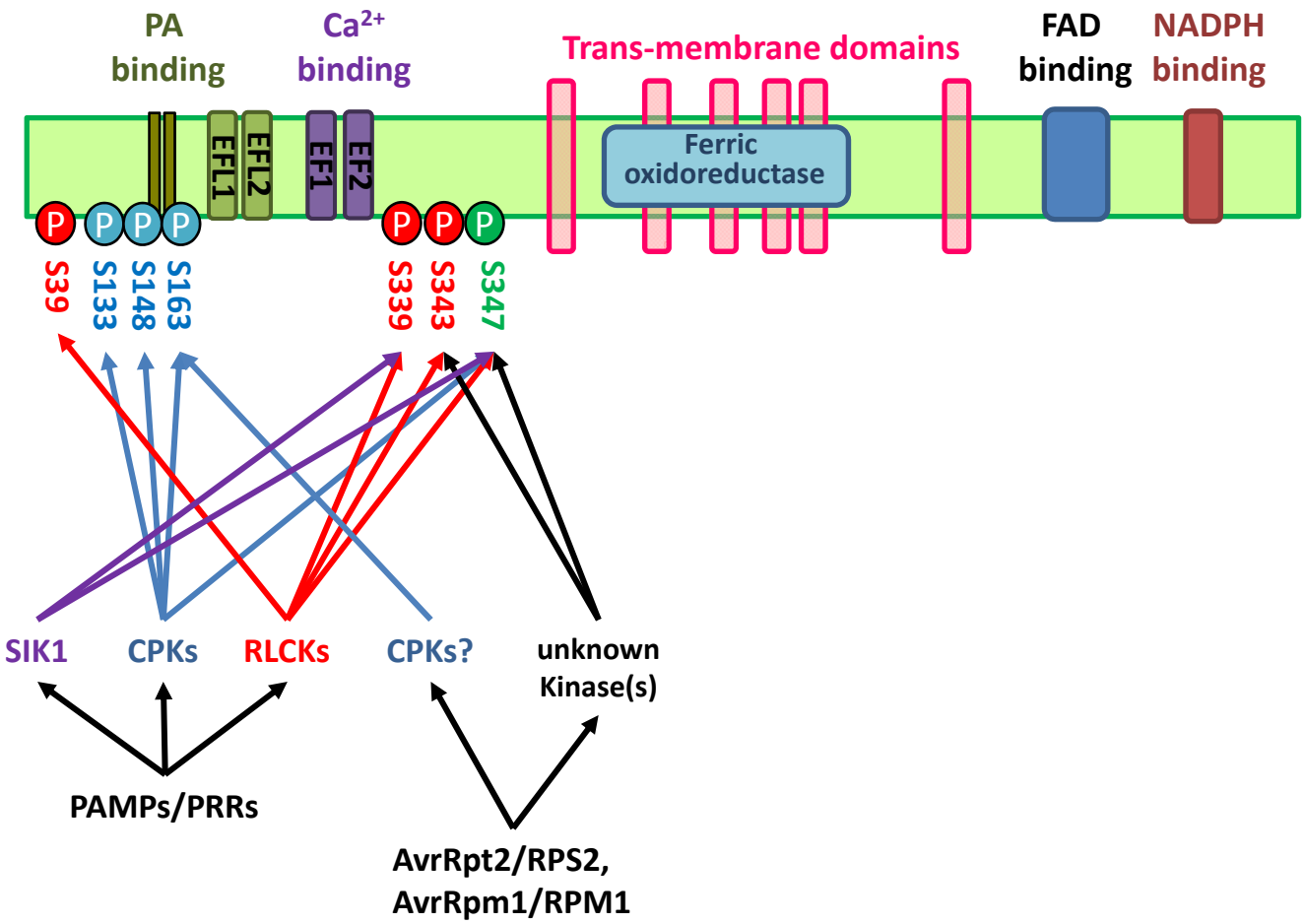

Fig. S6 Schematic representation of RESPIRATORY BURST OXIDASE HOMOLOGUE D (RBOHD) domains and phosphorylation sites significantly regulated during PAMP-triggered immunity (PTI) and effector-triggered immunity (ETI). RBOHD has two EF-hand motifs (EF1 and EF2), two EF-hand like motifs (EFL1 and EFL2) and possible phosphatidic acid (PA) binding sites in its N-terminal part, followed by six transmembrane domains encompassing the functional ferric oxidoreductase domain, one FAD-binding site, and one NADPH-binding site. During PTI, BIK1 phosphorylates residues S39, S339 and S343 (indicated in red), while CPKs phosphorylate residues S133, S148 and S163 (indicated in blue). MAP4K SIK1 also contributes to the phosphorylation on S339 and S347 during PTI. The residue S347 (indicated in green) is phosphorylated by both BIK1 and CPKs. We found that RESISTANT TO P. SYRINGAE-2 (RPS2) activation by AvrRpt2 induced phosphorylation at S163, S343, and S347. We validated that *Pseudomonas syringae* pv. *tomato* (*Pto*) DC3000 (*avrRpm1*) and *Pto* DC3000 (*avrRpt2*) induced phosphorylation at S343 and S347, while the kinase(s) phosphorylating these sites remain to be identified.